Microscopic Evidence of Charge- and Spin-Density Waves in $La_3Ni_2O_{7-\delta}$ Revealed by ^{139}La-NQR

Jun Luo(罗军)[1,2†], Jie Feng(冯杰)[1,2†], Gang Wang(王罡)[1,2], Ningning Wang(王宁宁)[1,2], Jie Dou(窦杰)[1,2], Aifang Fang(房爱芳)[3,4], Jie Yang(杨杰)[1,2], Jinguang Cheng(程金光)[1,2], Guoqing Zheng(郑国庆)[5], and Rui Zhou(周睿)[1,2*]

[1]*Institute of Physics, Chinese Academy of Sciences, and Beijing National Laboratory for Condensed Matter Physics, Beijing 100190, China*
[2]*School of Physical Sciences, University of Chinese Academy of Sciences, Beijing 100190, China*
[3]*School of Physics and Astronomy, Beijing Normal University, Beijing 100875, China*
[4]*Key Laboratory of Multiscale Spin Physics, Ministry of Education, Beijing Normal University, Beijing 100875, China*
[5]*Department of Physics, Okayama University, Okayama 700-8530, Japan*

(Received 17 March 2025; accepted manuscript online 30 April 2025)

The recent discovery of superconductivity in $La_3Ni_2O_{7-\delta}$ with a transition temperature T_c close to 80 K at high pressures has attracted significant attention, due particularly to a possible density wave (DW) transition occurring near the superconducting dome. Identifying the type of DW order is crucial for understanding the origin of superconductivity in this system. However, owing to the presence of $La_4Ni_3O_{10}$ and other intergrowth phases in $La_3Ni_2O_{7-\delta}$ samples, extracting the intrinsic information from the $La_3Ni_2O_7$ phase is challenging. In this study, we employed ^{139}La nuclear quadrupole resonance (NQR) measurements to eliminate the influence of other structural phases in the sample and obtain microscopic insights into the DW transition in $La_3Ni_2O_{7-\delta}$. Below the DW transition temperature $T_{DW} \sim 153$ K, we observe a distinct splitting in the $\pm5/2 \leftrightarrow \pm7/2$ transition of the NQR resonance peak at the La(2) site, while only a line broadening is seen in the $\pm3/2 \leftrightarrow \pm5/2$ transition peak. Through further analysis of the spectra, we show that the line splitting is due to a unidirectional charge modulation. A magnetic line broadening is also observed below T_{DW}, accompanied by a large enhancement of the spin-lattice relaxation rate, indicating the formation of magnetically ordered moments in the DW state. Our results suggest a simultaneous formation of charge- and spin-density wave orders in $La_3Ni_2O_{7-\delta}$, thereby offering critical insights into the electronic correlations in Ni-based superconductors.

DOI: 10.1088/0256-307X/42/6/067402 CSTR: 32039.14.0256-307X.42.6.067402

The mechanism of the cuprate high temperature superconductors is still under debate since their discovery.[1,2] Recently, $La_3Ni_2O_{7-\delta}$ shows superconductivity with the superconducting transition temperature T_c close to 80 K at $P > 14$ GPa,[3,4] generating a tremendous response from the research community and providing a new platform to study the mechanism of high temperature superconductivity.[5] $La_3Ni_2O_7$ (327) belongs to Ruddlesden–Popper (R–P) phases $La_{n+1}Ni_nO_{3n+1}$ with $n = 2$, including two NiO_6 octahedral layers separated by a La-O layer in the unit cell. Within the pressure range where superconductivity emerges, the structure concurrently changes from orthorhombic to tetragonal as revealed by X-ray diffraction (XRD).[3,6] Later, both the single crystal and polycrystalline samples achieve zero resistance at low temperatures.[7,8] However, due to the presence of La_2NiO_4 (214) and $La_4Ni_3O_{10}$ (4310) phases, as well as the intergrowth of different R–P phases observed by scanning transmission electron microscopy (STEM) and nuclear quadrupole resonance (NQR), the superconducting volume fraction is found to be less than 1% in $La_3Ni_2O_{7-\delta}$.[9,10] With Pr doping, both 4310 and intergrowth phases can be strongly suppressed, and the superconducting volume fraction can even exceed 90%.[10]

Not only the high transition temperature T_c, but another feature that a possible density wave (DW) state is adjacent to the superconducting phase is intriguing. This was initially observed through the abrupt change in the resistivity, Hall coefficient, and Seebeck coefficient at $T \sim 120$ K in $La_3Ni_2O_{7-\delta}$ under ambient pressure.[11,12] Subsequently, two transitions were detected by a recent electrical transport study in the single crystal sample, with transition temperatures of ∼110 K and 153 K, respectively.[13] Most intriguingly, transport measurements show that T_{DW} decreases with increasing pressure and disappears around 6 GPa, where superconductivity emerges.[8,14] Such behavior suggests a competition between the possible DW and superconducting states, which is similar to that in the cuprate superconductors.[2] We also note that a recent muon spin relaxation (μSR) study suggested that

†These authors contributed equally to this work.
*Corresponding author. Email: rzhou@iphy.ac.cn
© 2025 Chinese Physical Society and IOP Publishing Ltd. All rights, including for text and data mining, AI training, and similar technologies, are reserved.

the transition temperature $T_{\rm DW}$ rises with the increase of pressure.[15] In any case, an essential question arises regarding the existence of a DW order in $La_3Ni_2O_{7-\delta}$, and if it exists, whether it is a spin density wave (SDW) or a charge density wave (CDW). Or could it be a stripe order, where the spin and charge orders are coupled, as observed in $La_{2-x}Ba_xCuO_4$.[16] Various experimental methods have been utilized to investigate the nature of the possible DW state, but the results are contradictory. The appearance of the internal magnetic field in $La_3Ni_2O_{7-\delta}$ below $T \sim 150$ K, observed by μSR[15,17] and nuclear magnetic resonance (NMR),[18] points to a SDW order at low temperatures. This is also supported by the resonant inelastic X-ray scattering (RIXS), which reveals a quasi-static SDW order.[19] In all of these studies, it was found that the magnetic moment of Ni was rather small, only $\sim$0.5 $\mu_{\rm B}$/Ni. This implies that $La_3Ni_2O_{7-\delta}$ might differ from infinite-layer nickel oxide materials and does not present strong magnetic coupling.[20] The SDW could stem from the scattering between different sections of the Fermi surface. However, no long-range magnetic order was observed in neutron scattering (NS) measurements.[21] Other NMR measurements conducted on the polycrystal sample argued that the broadening of the NMR spectra is more associated with the CDW order.[22,23] The infrared spectroscopy investigation also supports the CDW order, but the CDW gap was found to be opened below $T \sim 115$ K.[24] The reason for these conflicting results can be attributed to the presence of multiple R–P phases in the $La_3Ni_2O_{7-\delta}$ samples, such as 4310 and 214 phases, as well as the intergrowth phases, as observed by the STEM and NQR measurements.[9,10] Especially, both SDW and CDW orders have been discovered by NS in $La_4Ni_3O_{10}$.[25] Therefore, it is of urgency to find a way to evade the influence of other phases and merely acquire the microscopic information of the 327 phase. Meanwhile, the investigation of the properties of the DW order is also essential for understanding the role of electron correlations and the superconducting mechanism in $La_3Ni_2O_7$, as recent angle-resolved photoemission spectroscopy and optical studies have suggested that the electron correlation might be relatively strong.[24,26,27]

In this study, we performed ^{139}La-NQR to study the DW order in $La_3Ni_2O_{7-\delta}$. Taking advantage of the NQR measurement, we can get rid of the influence of other R–P phases in the sample and extract the microscopic information related to the $La_3Ni_2O_7$ phase.[10] Below the DW transition temperature $T_{\rm DW} \sim 153$ K, a distinct line splitting is observed in the $\pm5/2 \leftrightarrow \pm7/2$ transition of the NQR resonance peak at the La(2) site, whereas only a line broadening is observed in the $\pm3/2 \leftrightarrow \pm5/2$ transition of the NQR resonance peak. Through further analysis of the spectra, we found that the line splitting is ascribed to the commensurate charge modulation, which is similar to the charge order in cuprates. A magnetic line broadening also emerges below $T_{\rm DW}$, indicating the formation of ordered moments. Meanwhile, a significant enhancement of the spin-lattice relaxation rate is further observed at $T_{\rm DW}$. All these findings suggest the simultaneous formation of spin- and charge-density wave orders in $La_3Ni_2O_{7-\delta}$ at the same temperature.

The polycrystalline sample of $La_3Ni_2O_{7-\delta}$ was synthesized by the sol-gel method,[8] and used in earlier work.[10] The oxygen stoichiometry parameter $\delta \approx 0.07$ was determined by thermogravimetric analysis. ^{139}La-NQR spectra were obtained by sweeping the frequency point by point, and integrating spin-echo intensity. The quantity of our sample used for NQR measurement is about 600 mg. The spin-lattice relaxation time T_1 was measured by the saturation-recovery method. Because η is close to zero, we ignore the influence of η on the recovery curve.

In the crystal structure of $La_3Ni_2O_7$ shown in Fig. 1(a), there are two types of La sites. Namely, La(1) sites are located inside the NiO_2 bilayer, and La(2) sites are outside the NiO_2 bilayer. The Hamiltonian caused by quadrupole interaction at zero field is $\mathcal{H}_Q = \frac{e^2qQ}{4I(2I-1)}[(3I_z^2 - I^2) + \frac{1}{2}\eta(I_+^2 + I_-^2)]$.[28] $eq = V_{ZZ} = \frac{\partial^2 V}{\partial Z^2}$ is the electric field gradient (EFG) along the principal axis and V is the electric potential, Q is the nuclear quadrupole moment, and $\eta = |(V_{XX} - V_{YY})/V_{ZZ}|$ is the asymmetry parameter of EFG. The nuclear quadrupole resonance frequency ν_Q is defined as $\frac{3e^2qQ}{2I(2I-1)h}$. For the ^{139}La nucleus with spin 7/2, the NQR spectrum should have three resonance peaks corresponding to $\pm1/2 \leftrightarrow \pm3/2$, $\pm3/2 \leftrightarrow \pm5/2$, and $\pm5/2 \leftrightarrow \pm7/2$ transitions. Thus, a total of six sets of peaks should be observed in the ^{139}La-NQR spectrum for $La_3Ni_2O_7$. However, the ν_Q of La(1) is only 2.2 MHz.[10,18,22,23] Hence, we only observe two sets of resonance peaks in the NQR spectra corresponding to the La(2) site between 10 to 19 MHz as shown in Fig. 1(b). At $T = 188$ K, each set exhibits four peaks in the La(2) NQR spectrum [Fig. 1(b), top], indicating the presence of four distinct La(2) sites. Based on the previous STEM and

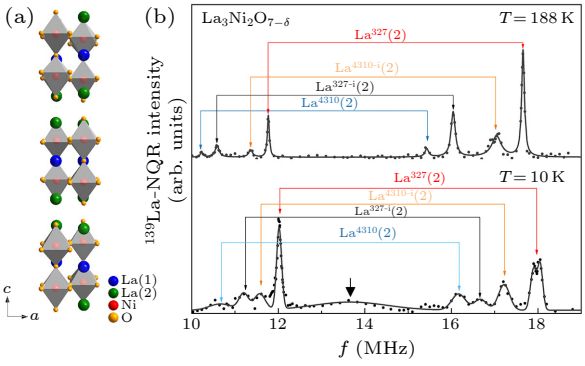

Fig. 1. (a) The crystal structure of $La_3Ni_2O_7$ at ambient pressure. (b) The ^{139}La-NQR spectra at 188 K and 10 K, respectively. There are two sets of resonance peaks, corresponding to $\pm5/2 \leftrightarrow \pm7/2$ and $\pm3/2 \leftrightarrow \pm5/2$ transitions within the range of 10 MHz to 19 MHz. The two resonance peaks between the peaks of $La^{4310}(2)$ and $La^{327}(2)$ are from $La^{327\text{-i}}(2)$ and $La^{4310\text{-i}}(2)$ sites, which correspond to the La(2) sites from the intergrowth between 327 and 4310 phases (see Fig. S1 in Supplementary Materials (SM)). The solid arrow represents the broad peak corresponding to the La_2NiO_4 phase. At 188 K and 10 K, the spectra are respectively fitted by Lorentz and Gaussian functions (solid lines).

NQR study,[10] we can ascribe the lowest-frequency peak to the 4310 phase. The two intermediate peaks originate from two sites within the intergrowth between the 327 and 4310 phases (see Fig. S1 in SM). Nevertheless, in the previous NQR study,[10] $1/T_1T$ measurements were not carried out, and the lower-frequency peak was assumed to be $La^{4310\text{-i}}(2)$. From the temperature dependence of the $1/T_1T$ results at different peaks (see Fig. S5 in SM), we are now able to assign the resonance peaks, from low to high frequency, to the $La^{4310}(2)$, $La^{327\text{-i}}(2)$, $La^{4310\text{-i}}(2)$, and $La^{327}(2)$ sites.

With decreasing temperature below $T_{\rm DW}$, a clear splitting appears at $La^{327}(2)$ site of the $\pm5/2 \leftrightarrow \pm7/2$ transition, while line broadening can be seen at other sites [see Fig. 1(b), bottom]. A broad peak at ∼13 MHz is observed below $T = 30$ K (see Fig. S4 in SM). Considering that the 214 phase was detected by STEM in the polycrystal sample,[10] and a similar broad peak was observed in the previous NQR study,[29] we ascribe this broad peak to the 214 phase. In order to obtain the intrinsic information from the 327 phase, we thus focus on the $La^{327}(2)$ site. Figure 2(a) presents the temperature dependence of the resonance peak of the $La^{327}(2)$ site corresponding to the $\pm5/2 \leftrightarrow \pm7/2$ transition. Below $T_{\rm DW} \sim 153$ K, the peak begins to broaden and further splits at low temperatures. For the $La^{327}(2)$ NQR spectra corresponding to the $\pm3/2 \leftrightarrow \pm5/2$ transition, only the line broadening can be observed down to 10 K (see Fig. S2 in SM). Then we fit the $La^{327}(2)$ spectra corresponding to $\pm3/2 \leftrightarrow \pm5/2$ and $\pm5/2 \leftrightarrow \pm7/2$ transitions with two Gaussian functions below $T_{\rm DW}$ (see Fig. S2 in SM), and obtain the interval of the two splitting lines $\Delta\nu$ as shown in Fig. 2(b). A rapid increase of $\Delta\nu$ just below $T_{\rm DW}$ is seen for both $\pm3/2 \leftrightarrow \pm5/2$ and $\pm5/2 \leftrightarrow \pm7/2$ transitions. Meanwhile, a significant enhancement of $1/T_1$ with the decrease of temperature down to $T_{\rm DW}$ is also observed as shown in Fig. 2(c). The increase of $1/T_1$ from $T \sim 180$ K down to $T_{\rm DW}$ is due to the fluctuations of the possible DW order. Below $T_{\rm DW}$, $1/T_1$ is measured at both splitting lines, and both are found to decrease with the decrease of temperature due to the gap opening. All these indicate the appearance of a DW phase transition at $T_{\rm DW}$. The $1/T_1T$ below 50 K decreases to 1% of that at high temperatures above $T_{\rm DW}$, suggesting that most parts of the Fermi surface are gapped. Furthermore, we also note that the temperature dependence of $1/T_1T$ results at the $La^{4310\text{-i}}(2)$ site suggests that the $T_{\rm DW} \sim 133$ K of the intergrowth 4310 phase is still close to the transition temperature of the pure 4310 phase identified in previous NS studies (see Fig. S5 in SM).[25] This explains why two DW transitions can occasionally be detected in the $La_3Ni_2O_7$ sample through electrical resistivity measurements.[13]

The observed line splitting can be due to either an emergence of an internal magnetic field or a modulation of the charge density. As previously indicated by NMR measurements, the principal axis of the EFG for the La site is along the c axis.[18] Then, in the case where the internal magnetic field $B_{\rm int}$ is along the c axis due to the SDW order, the NQR line splitting should be $2\gamma B_{\rm int}$ for all transitions [see Fig. 3(a)], where $\gamma = 6.0146$ MHz/T is the nuclear gyromagnetic ratio of ^{139}La.

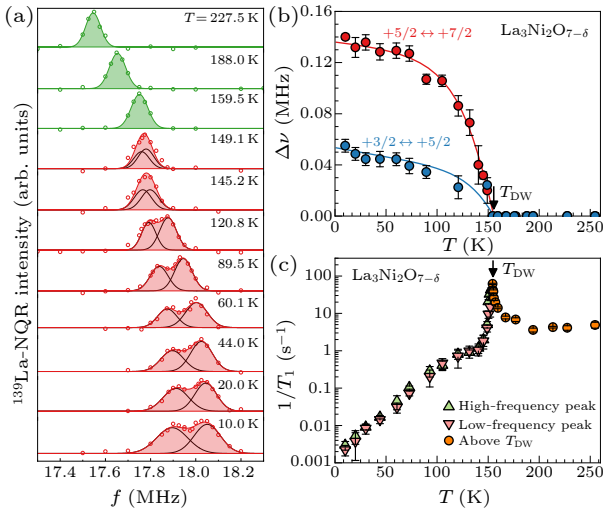

Fig. 2. (a) The temperature dependence of the $La^{327}(2)$ NQR spectra corresponding to the $\pm5/2 \leftrightarrow \pm7/2$ transition. Above $T_{\rm DW}$, the NQR spectra are fitted with one Gaussian function. Below $T_{\rm DW}$, the NQR spectra are fitted with two Gaussian functions. (b) Temperature dependence of the NQR line splitting of both $\pm3/2 \leftrightarrow \pm5/2$ and $\pm5/2 \leftrightarrow \pm7/2$ transitions obtained from the fitting of the NQR spectra (see Fig. S3 in SM for details). Below the DW phase transition, the NQR line splitting $\Delta\nu$ increases rapidly with decreasing temperature. (c) Temperature dependence of $1/T_1$ measured at the $\pm5/2 \leftrightarrow \pm7/2$ transition. The black arrows represent $T_{\rm DW}$.

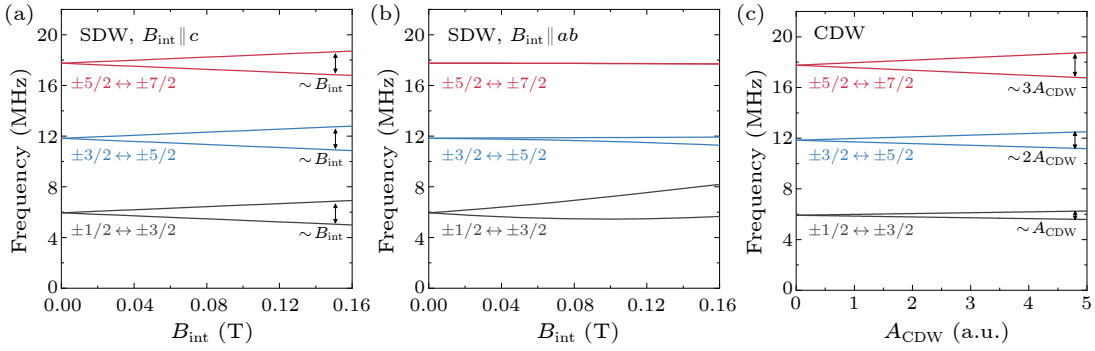

Fig. 3. The calculated evolution of the NQR lines in the presence of the internal field along the c axis (a) and ab plane (b) for the La(2) site. (c) The calculated evolution of the NQR lines in the presence of the CDW order as functions of the amplitude of the charge modulation. For all calculations, ν_Q and η are taken as 5.92 MHz and 0.04, respectively.

We would expect to observe that $\Delta\nu$ at both $\pm3/2 \leftrightarrow \pm5/2$ and $\pm5/2 \leftrightarrow \pm7/2$ transitions is identical. For the case of the internal magnetic field $B_{\rm int}$ along the ab plane from the SDW order as suggested by previous NMR and RIXS studies,[18,19] the NQR line splitting at the $\pm5/2 \leftrightarrow \pm7/2$ transition should be barely seen and much smaller than the line splitting at the $\pm3/2 \leftrightarrow \pm5/2$ transition [see Fig. 3(b)]. Therefore, our results imply that the NQR line splitting unlikely originates from the SDW order.

For the case of the charge modulation, the NQR line splitting should be proportional to the NQR frequency. We would expect to observe that $\Delta\nu$ at $\pm5/2 \leftrightarrow \pm7/2$ transition should be 1.5 times larger than that of $\pm3/2 \leftrightarrow \pm5/2$ [see Fig. 3(c)], when the η of two La(2) sites is the same. As shown in Fig. 2(b), $\Delta\nu$ of the $\pm5/2 \leftrightarrow \pm7/2$ transition is about 2 times larger than that of the $\pm3/2 \leftrightarrow \pm5/2$, which is slightly larger than the expected value of 1.5. It is possible that the EFG asymmetry parameter η of the two splitting lines is not identical, or that there exists a very small internal magnetic field along the ab plane at La(2) sites. All these could lead to the observed $\Delta\nu$ ratio between $\pm5/2 \leftrightarrow \pm7/2$ and $\pm3/2 \leftrightarrow \pm5/2$ being slightly larger than the expected value of 1.5. In any case, our observation still indicates that the observed splitting is mainly attributed to the charge modulation resulting from a CDW order below $T_{\rm DW}$. Such behavior is similar to the previously observed phenomena in cuprates[30,31] and kagome metals.[32] To obtain the precise parameters from the NQR measurements, narrower lines from high-quality single crystals and measurements on the $\pm1/2 \leftrightarrow \pm3/2$ transition are required in the future.

For the one-dimensional (1D) incommensurate CDW order,[33,34] the NMR spectrum is expected to have two peaks of equal intensities, and most importantly, a continuum between the two peaks. In the cases of 2D or 3D, if the amplitude of the charge modulation along one direction is much stronger than the others, the NMR spectrum should be similar to that of the 1D incommensurate CDW order. Otherwise, the spectrum should only have one symmetric peak, which is not consistent with our observation. Considering a line splitting in our spectra within the CDW state, we then simulate the NQR spectra at 10 K (see Fig. S8 of SM). We find that the fitting of two Gaussian functions is more consistent with our experimental results than the simulation of 1D incommensurate CDW order, suggesting that the charge modulation is commensurate. Then the two peaks of ^{139}La-NQR spectra indicate that there are two types of La(2) sites in the CDW state. Considering that La(2) is at the center of four nearby Ni atoms, we propose two possible charge modulation patterns as shown in Fig. 4. The first possible CDW pattern is the double charge stripe order [see Fig. 4(a)]. In this CDW state, there are two types of La(2) sites arranged in a zigzag chain. This CDW pattern is consistent with the CDW-Z1 mode proposed in a previous theoretical work,[35] where the CDW was proposed to be induced by the tendency of structural distortion due to the four imaginary modes existing in the phonon spectrum at ambient pressure. Another possible CDW pattern is shown in Fig. 4(b),

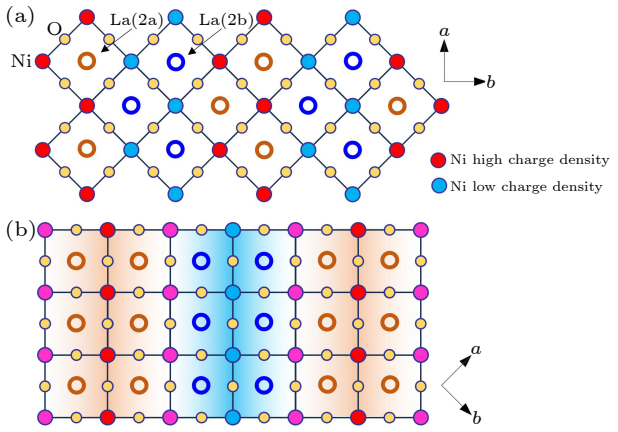

Fig. 4. Illustration of possible CDW patterns below $T_{\rm DW}$. The double charge stripe order and the unidirectional CDW along the Ni-O-Ni bond direction compatible with the NQR spectra are shown in (a) and (b). The red (blue) solid circle represents Ni with high (low) charge density. The open circles represent two La(2) sites, marked as La(2a) and La(2b). The light orange and light blue shades indicate high charge density and low charge density area in (b).

in which the stripe-type charge modulation is along the Ni-O-Ni bond direction. In this case, there are also two types of La(2) sites. This type of CDW is similar to long-range commensurate CDW order in $Bi_2Sr_2CaCu_2O_{8+x}$[36] and $YBa_2Cu_3O_y$.[37] In any case, our results suggest that the CDW order is commensurate and unidirectional. In principle, additional diffraction peaks should be observable by X-ray scattering due to charge modulation; however, this was not observed so far.[19] This might be attributed to the fact that X-ray scattering, as a bulk measurement, is influenced by the presence of other structural phases, such as 4310, 214, and other intergrowth phases, which would blur the signature of the charge modulation.

We can further obtain information in the DW state from the temperature dependence of the full width at half maximum (FWHM), including both high- and low-frequency peaks of two split peaks below $T_{\rm DW}$ and a single peak above $T_{\rm DW}$ (see Fig. S6 in SM). Above $T_{\rm DW}$, the FWHM is independent of temperature, but it starts to increase below $T_{\rm DW}$ for both $\pm5/2 \leftrightarrow \pm7/2$ and $\pm3/2 \leftrightarrow \pm5/2$ transitions. In principle, the broadening of the NQR spectrum can be attributed to both quadrupole and magnetic contributions. The FWHM can be expressed by an *ad hoc* formula, $w_{\rm tot} = \sqrt{(m \cdot w_{\rm quad})^2 + (w_{\rm mag})^2}$. The $w_{\rm quad}$ and $w_{\rm mag}$ are the quadrupole and magnetic contributions to the line broadening. The value of m is 2 for the $\pm3/2 \leftrightarrow \pm5/2$ transition and 3 for the $\pm5/2 \leftrightarrow \pm7/2$ transition, respectively. Therefore, we can deduce the magnetic contribution $w_{\rm mag}$ and the quadrupole contribution $w_{\rm quad}$ from the total FWHM $w_{\rm tot}$, as shown in Figs. 5(a) and 5(b), respectively. Above $T_{\rm DW}$, the magnetic broadening $w_{\rm mag}$ is nearly zero. However, $w_{\rm mag}$ of both high- and low-frequency peaks of the two split peaks starts to increase below $T_{\rm DW}$, becoming the dominant contribution to the total FWHM at low temperatures. In contrast, the quadrupole contribution $w_{\rm quad}$ remains almost temperature-independent within the DW state.

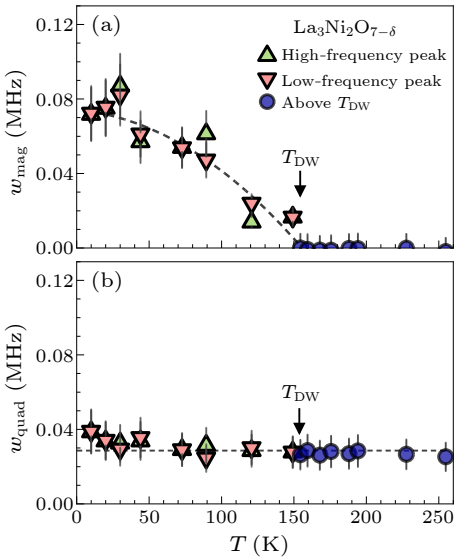

Fig. 5. The magnetic (a) and quadrupole (b) contribution to the FWHM extracted from the total FWHM (see Fig. S6 in SM for details), including both high- and low-frequency peaks of two split peaks below T_{DW} and a single peak above T_{DW}. The black arrows represent T_{DW}. The dashed lines are the guides to the eye.

The emergence of magnetic broadening at zero field indicates the formation of a magnetic ordered moment associated with the spin density wave in $La_3Ni_2O_7$. Meanwhile, we observe that $1/T_1$ is T-independent at high temperatures above $T \sim 180$ K but increases by nearly two orders of magnitude at T_{DW} in $La_3Ni_2O_7$ [see Fig. 2(c)]. Such behavior contrasts with the situation in kagome metals where $1/T_1$ decreases as the temperature drops down to the CDW transition temperature.[32] The T-independent $1/T_1$ at high temperatures is consistent with the existence of local magnetic moments,[38] and resembles previous observations in $La_{2-x}Sr_xCuO_4$ near the spin ordering transition.[39,40] All these indicate that the enhancement of $1/T_1$ originates from spin fluctuations, providing further evidence for the presence of SDW order below T_{DW}.

In NQR measurements, since no external magnetic field is applied and polycrystalline samples are used, the line broadening might arise from the distribution of magnetic moments in any direction due to the oxygen content distribution within the sample. Consequently, we cannot provide more information about the structure of the SDW order. However, we note that the observed internal field B_{int} at the La(2) site can be estimated from the magnetic line broadening as $B_{int} \sim 0.005$ T, which is close to half of the B_{int} at the La(1) site.[18] Considering that the La(1) site is between two NiO_2 layers and the La(2) site is only close to one NiO_2 layer, the observed B_{int} value suggests that our observation is consistent with the NMR measurements.[18] Moreover, the small B_{int} led to only broadening being observed in the NQR spectra, rather than splitting. The double spin stripe is proposed for the structure of the SDW order by previous NMR and RIXS studies.[18,19] Our results further imply that the double charge stripe could be a possible structure of the CDW order. Therefore, in combination with the previous study on the SDW order, all these suggest that the CDW and SDW might be coupled in $La_3Ni_2O_7$, similar to the stripe order in $La_{2-x}Ba_xCuO_4$.[16] Meanwhile, the commensurate nature of the CDW order is also similar to that of the cuprates.[36,37] However, there is a striking difference between Ni-based compounds and the cuprates. In the latter, the undoped parent compound is a Mott insulator, but the former is not, with an electrical conductivity worse than the kagome metal, though.[41] In the parent cuprates such as La_2CuO_4, the internal magnetic field due to the antiferromagnetic interaction is huge, with the hyperfine field about 0.1 T at the La-site,[42] which is much larger than we found here. Although CDW is also present in the cuprates, except at a particular doping rate of 1/8, the order is only short range, which can be stabilized to become long range only after applying a strong magnetic field[30,31] or uniaxial strain.[43,44] By contrast, the CDW long-range order is robust already in the undoped nickelates. Furthermore, we notice that $La_3Ni_2O_7$ bears similarities to the trilayer compound $La_4Ni_3O_{10}$, in which both CDW and SDW occur simultaneously. One possibility is that the SDW emerges from Fermi surface nesting.[45,46] Subsequently, spin-lattice coupling might concurrently induce charge ordering, offering a potential mechanism for the coexistence of charge and magnetic order.[47] Additionally, it is also possible that $La_3Ni_2O_7$ is similar to $La_4Ni_3O_8$,[48] where spin and charge stripes are strongly coupled,[49] and neither order parameter is secondary. In any case, our results thus provide new perspectives for the study of high-temperature superconductors and can stimulate more theoretical and experimental investigations.

In summary, we have performed ^{139}La-NQR to eliminate the influence of other R–P phases and obtain the microscopic information related to the DW transition in $La_3Ni_2O_{7-\delta}$. Below the DW transition temperature $T_{DW} \sim 153$ K, a distinct line splitting is observed in the $\pm 5/2 \leftrightarrow \pm 7/2$ transition of the NQR resonance peak at the La(2) site, indicating the unidirectional CDW order. Meanwhile, $1/T_1$ is T-independent at high temperatures but is largely enhanced towards T_{DW} upon cooling, with an emergence of magnetic broadening below T_{DW}, pointing to the formation of magnetic ordered moments in the DW state. All these findings indicate the formation of CDW and SDW orders in $La_3Ni_2O_{7-\delta}$ simultaneously. Our results elucidate the nature of the DW order, thereby furnishing crucial information for understanding the electronic correlations in Ni-based high-temperature superconductors.

Acknowledgments. This work was supported by the National Key Research and Development Projects of China (Grant Nos. 2023YFA1406103, 2024YFA1611302, 2024YFA1409200, and 2022YFA1403402), the National Natural Science Foundation of China (Grant Nos. 12374142, 12304170, 12025408, 12404179, and U23A6003), Beijing National Laboratory for Condensed Matter Physics (Grant No. 2024BNLCMPKF005), and

the Chinese Academy of Sciences President's International Fellowship Initiative (Grant No. 2024PG0003). This work was also supported by the Synergetic Extreme Condition User Facility (SECUF, https://cstr.cn/31123.02.SECUF).

References

[1] Lee P A, Nagaosa N, and Wen X G 2006 *Rev. Mod. Phys.* **78** 17

[2] Keimer B, Kivelson S A, Norman M R, Uchida S, and Zaanen J 2015 *Nature* **518** 179

[3] Sun H L, Huo M W, Xu X W, Li J Y, Liu Z J, Han Y F, Tang L Y, Mao Z Q, Yang P T, Wang B S, Cheng J G, Yao D X, Zhang G M, and Wang M 2023 *Nature* **621** 493

[4] Hou J, Yang P T, Liu Z Y, Li J Y, Shan P F, Ma L, Wang G, Wang N N, Guo H Z, Sun J P, Uwatoko Y, Wang M, Zhang G M, Wang B S, and Cheng J G 2023 *Chin. Phys. Lett.* **40** 117302

[5] Wang M, Wen H H, Wu T, Yao D X, and Xiang T 2024 *Chin. Phys. Lett.* **41** 077402

[6] Wang L H, Li Y, Xie S Y, Liu F Y, Sun H L, Huang C X, Cao Y, Nakagawa T, Fu B Y, Dong B, Cao Z H, Yu R Z, Kawaguchi S I, Kadobayashi H, Wang M, Jin C Q, Mao H K, and Liu H Z 2024 *J. Am. Chem. Soc.* **146** 7506

[7] Zhang Y N, Su D J, Huang Y E, Shan Z Y, Sun H L, Huo M W, Ye K X, Zhang J W, Yang Z H, Xu Y K, Su Y, Li R, Smidman M, Wang M, Jiao L, and Yuan H Q 2024 *Nat. Phys.* **20** 1269

[8] Wang G, Wang N N, Shen X L, Hou J, Ma L, Shi L F, Ren Z A, Gu Y D, Ma H M, Yang P T, Liu Z Y, Guo H Z, Sun J P, Zhang G M, Calder S, Yan J Q, Wang B S, Uwatoko Y, and Cheng J G 2024 *Phys. Rev. X* **14** 011040

[9] Zhou Y Z, Guo J, Cai S, Sun H L, Li C Y, Zhao J Y, Wang P Y, Han J Y, Chen X T. Chen Y J, Wu Q, Ding Y, Xiang T, Mao H K, and Sun L L 2025 *Matter Radiat. Extremes* **10** 027801

[10] Wang N N, Wang G, Shen X L, Hou J, Luo J, Ma X P, Yang H X, Shi L F, Dou J, Feng J, Yang J, Shi Y Q, Ren Z A, Ma H M, Yang P T, Liu Z Y, Liu Y, Zhang H, Dong X L, Wang Y X, Jiang K, Hu J P, Nagasaki S, Kitagawa K, Calder S, Yan J Q, Sun J P, Wang B S, Zhou R, Uwatoko Y, and Cheng J G 2024 *Nature* **634** 579

[11] Sreedhar K, McElfresh M, Perry D, Kim D, Metcalf P, and Honig J M 1994 *J. Solid State Chem.* **110** 208

[12] Taniguchi S, Nishikawa T, Yasui Y, Kobayashi Y, Takeda J, Shamato S, and Sato M 1995 *J. Phys. Soc. Jpn.* **64** 1644

[13] Liu Z J, Sun H L, Huo M W, Ma X Y, Ji Y, Yi E K, Li L S, Liu H, Yu J, Zhang Z Y, Chen Z Q, Liang F X, Dong H L, Guo H J, Zhong D Y, Shen B, Li S L, and Wang M 2023 *Sci. China Phys. Mech. Astron.* **66** 217411

[14] Wu G Q, Neumeier J J, and Hundley M F 2001 *Phys. Rev. B* **63** 245120

[15] Khasanov R, Hicken T J, Gawryluk D J, Sazgari V, Plokhikh I, Sorel L P, Bartkowiak M, Bötzel S, Lechermann F, Eremin I M, Luetkens H, and Guguchia Z 2025 *Nat. Phys.* **21** 430

[16] Tranquada J M, Sternlieb B J, Axe J D, Nakamura Y, and Uchida S 1995 *Nature* **375** 561

[17] Chen K W, Liu X Q, Jiao J C, Zou M Y, Jiang C Y, Li X, Luo Y X, Wu Q, Zhang N Y, Guo Y F, and Shu L 2024 *Phys. Rev. Lett.* **132** 256503

[18] Zhao D, Zhou Y B, Huo M W, Wang Y, Nie L P, Yang Y, Ying J J, Wang M, Wu T, and Chen X H 2025 *Sci. Bull.* **70** 1239

[19] Chen X Y, Choi J, Jiang Z C, Mei J, Jiang K, Li J, Agrestini S, Garcia-Fernandez M, Sun H L, Huang X, Shen D W, Wang M, Hu J P, Lu Y, Zhou K J, and Feng D L 2024 *Nat. Commun.* **108** 9597

[20] Cui Y, Li C, Li Q, Zhu X Y, Hu Z, Yang Y F, Zhang J S, Yu R, Wen H H, and Yu W Q 2021 *Chin. Phys. Lett.* **38** 067401

[21] Xie T, Huo M W, Ni X S, Shen F R, Huang X, Sun H L, Walker H C, Adroja D, Yu D H, Shen B, He L H, Cao K, and Wang M 2024 *Sci. Bull.* **69** 3221

[22] Fukamachi T, Oda K, Kobayashi Y, Miyashita T, and Sato M 2001 *J. Phys. Soc.Jpn.* **70** 2757

[23] Kakoi M, Oi T, Ohshita Y, Yashima M, Kuroki K, Kato T, Takahashi H, Ishiwata S, Adachi Y, Hatada N, Uda T, and Mukuda H 2024 *J. Phys. Soc. Jpn.* **93** 053702

[24] Liu Z, Huo M W, Li J, Li Q, Liu Y C, Dai Y M, Zhou X X, Hao J H, Lu Y, Wang M, and Wen H H 2024 *Nat. Commun.* **15** 7570

[25] Zhang J J, Phelan D, Botana A S, Chen Y S, Zheng H, Krogstad M, Wang S G, Qiu Y M, Rodriguez-Rivera J A, Osborn R, Rosenkranz S, Norman M R, and Mitchell J F 2020 *Nat. Commun.* **11** 6003

[26] Yang J G, Sun H L, Hu X W, Xie Y Y, Miao T M, Luo H L, Chen H, Liang B, Zhu W P, Qu G X, Chen C Q, Huo M W, Huang Y B, Zhang S J, Zhang F F, Yang F, Wang Z M, Peng Q J, Mao H Q, Liu G D, Xu Z Y, Qian T, Yao D X, Wang M, Zhao L, and Zhou X J 2024 *Nat. Commun.* **15** 4373

[27] Geisler B, Fanfarillo L, Hamlin J J, Stewart G R, Hennig R G, and Hirschfeld P J 2024 *npj Quan. Mater.* **9** 89

[28] Abragam A 1961 *The Principles of Nuclear Magnetism* (Oxford Univ. Press, Oxford)

[29] Wada S, Kobayashi T, Kaburagi M, Shibutani K, and Ogawa R 1989 *J. Phys. Soc. Jpn.* **58** 2658

[30] Wu T, Mayaffre H, Krämer S, Horvatić M, Berthier C, Hardy W N, Liang R X, Bonn D A, and Julien M H 2011 *Nature* **477** 191

[31] Kawasaki S, Li Z, Kitahashi M, Lin C T, Kuhns P L, Reyes A P, and Zheng G Q 2017 *Nat. Commun.* **8** 1267

[32] Luo J, Zhao Z, Zhou Y Z, Yang J, Fang A F, Yang H T, Gao H J, Zhou R, and Zheng G Q 2022 *npj Quan. Mater.* **7** 30

[33] Blinc R and Apih T 2002 *Prog. Nucl. Mag. Res. Sp.* **41** 49

[34] Feng X Y, Zhao Z, Luo J, Yang J, Fang A F, Yang H T, Gao H J, Zhou R, and Zheng G Q 2023 *npj Quan. Mater.* **8** 23

[35] Yi X W, Meng Y, Li J W, Liao Z W, Li W, You J Y, Gu B, and Su G 2024 *Phys. Rev. B* **110** L140508

[36] Mesaros A, Fujita K, Edkins S D, Hamidian M H, Eisaki H, Uchida S I, Davis J C S, Lawler M J, and Kim E A 2016 *Proc. Nat. Acad. Sci.* **113** 12661

[37] Vinograd I, Zhou R, Hirata M, Wu T, Mayaffre H, Krämer S, Liang R X, Hardy W N, Bonn D A, and Julien M H 2021 *Nat. Commun.* **12** 3274

[38] Moriya T 1956 *Prog. Theor. Phys.* **16** 641

[39] Arsenault A, Takahashi S K, Imai T, He W, Lee Y S, and Fujita M 2018 *Phys. Rev. B* **97** 064511

[40] Frachet M, Vinograd I, Zhou R, Benhabib S, Wu S F, Mayaffre H, Krämer S, Ramakrishna S K, Reyes A P, Debray J, Kurosawa T, Momono N, Oda M, Komiya S, Ono S, Horio M, Chang J, Proust C, LeBoeuf D, and Julien M H 2020 *Nat. Phys.* **16** 1064

[41] Wilson S D and Ortiz B R 2024 *Nat. Rev. Mater.* **9** 420

[42] Kitaoka Y, Ishida K, Hiramatsu S, and Asayama K 1988 *J. Phys. Soc. Jpn.* **57** 734

[43] Kim H H, Souliou S M, Barber M E, Lefrancois E, Minola M, Tortora M, Heid R, Nandi N, Borzi R A, Garbarino G, Bosak A, Porras J, Loew T, König M, Moll P J W, Mackenzie A P, Keimer B, Hicks C W, and Tacon M L 2018 *Science* **362** 1040

[44] Kawasaki S, Tsukuda N, Lin C T, and Zheng G Q 2024 *Nat. Commun.* **15** 5082

[45] Lechermann F, Bötzel S, and Eremin I M 2024 *Phys. Rev. Mater.* **8** 074802

[46] Wang Y X, Jiang K, Wang Z Q, Zhang F C, and Hu J P 2024 *Phys. Rev. B* **110** 205112

[47] Ni X S, Ji Y Y, He L X, Xie T, Yao D X, Wang M, and Cao K 2025 *npj Quan. Mater.* **10** 17

[48] Zhang J J, Pajerowski D M, Botana A S, Zheng H, Harriger L, Rodriguez-Rivera J, Ruff J P C, Schreiber N J, Wang B, Chen Y S, Chen W C, Norman M R, Rosenkranz S, Mitchell J F, and Phelan D 2019 *Phys. Rev. Lett.* **122** 247201

[49] Mochizuki Y, Akamatsu H, Kumagai Y, and Oba F 2018 *Phys. Rev. Mater.* **2** 125001